

EVALUATION OF REMOTELY SENSED RAINFALL ALGORITHMS FOR STRONG HURRICANES

**E. Mahani S.¹, Nourozi N.², J. Kuligowski R.³,
Khanbilvardi R.⁴, Hsu K.⁵ and Nazari R.⁶**

¹*Investigator and Assistant Professor, Civil Engineering Department and NOAA-CREST Center at the City College of the City University of New York (CUNY), New York, NY, USA*

²*Investigator, NOAA-CREST Center and Civil Engineering Department at the City College of the City University of New York (CUNY), New York, NY, USA*

³*Investigator, NOAA/National Environmental Satellite, Data, and Information Service (NESDIS)-STAR, Camp Springs, MD, USA*

⁴*Professor, NOAA-CREST Center and Civil Engineering Department at the City College of the City University of New York (CUNY), New York, NY, USA*

⁵*Investigator, Center for Hydrometeorology and Remote Sensing (CHRS), Department of Civil and Environmental Engineering, University of California, Irvine (UCI), Irvine, CA, USA*

⁶*Investigator, NOAA-CREST Center and Civil Engineering Department at the New York City College of Technology, the City University of New York (CUNY), New York, NY, USA*

Received: 23rd March 2018 Revised: 14th April 2018 Accepted: 10th September 2018

ABSTRACT: Quantifying the accuracy of precipitation products has numerous benefits, including helping algorithm developers to improve their techniques and helping users to understand the reliability of the remotely sensed model estimates. The objective of the present study is to validate several satellite-based rainfall retrieval algorithms which use infrared (IR) or combination of IR with other frequencies for strong hurricanes after making landfall in order to identify areas of potential algorithm improvements. Four satellite-based rainfall algorithms are selected to be evaluated: the Hydro-Estimator (HE), GOES Multi Spectral Rainfall Algorithm (GMSRA), Remotely Sensing Information using an Artificial Neural Network System with Cloud Classification Scheme (PERSIANN-CCS), and Tropical Rainfall Measuring Mission (TRMM) Multi-satellite Precipitation Analysis (TMPA)-3B42RT. Validation of these algorithms' products has been performed against rain gauge-adjusted radar-based rainfall, NEXt generation RADar (NEXRAD) Stage-IV, for five land-falling hurricanes: Charley, Frances, Jeanne, Rita, and Wilma in 2004 and 2005. The results of this study concluded that the Hydro-Estimator could detect the rain bands of hurricanes much better than the other satellite based algorithms, but PERSIANN-CCS and TMPA-3B42 could capture the overall rainfall patterns as a whole better than the other algorithms. GMSRA, in general, produces the lowest intensity and the lowest correlation against Stage-IV.

Keywords: Validation, Hurricane, Satellite-based rainfall, Hydro-Estimator; PERSIANN-CCS; GMSRA, TMPA-3B42, Stage-IV, Radar rainfall, Comparison.

1. INTRODUCTION

Accurate precipitation information, particularly from severe storms (e.g., hurricanes), is critical for applications covering the entire range of the hydrologic cycle – flood forecasting, water resources management, water budget studies, and so on. As many authors have noted, however, precipitation is highly variable in time and space [1, 2] and [3] even at regional scale [4] and

thus is one of the most difficult atmospheric variables to measure with an accuracy that is acceptable for most hydro-meteorological applications. Several different methods for measuring/estimating rainfall offer complementary information with different scales, strengths, and weaknesses. Rain gauge measurements are the most accurate and represent a direct measurement but at point-based not areal coverage, hence spatial representativeness errors can be significant. Ground-based radars provide spatially distributed area-average estimates, but beam blockage, beam overshoot, and other factors limit the effective coverage of the observations. Satellite techniques provide uninterrupted spatial coverage, which is a great advantage, particularly covering regions that are inaccessible by other observing systems such as rain gauges and ground-based radar systems.

Another advantage of using satellite information in comparison with ground-based radar systems, besides uninterrupted spatial coverage, is that the satellite is out of reach of severe and extreme events (e.g., earthquakes and hurricanes). As an example, significant portion of the radar data are missing in Fig. 1 (left), because Hurricane Katrina caused loss of power and communications to the Lower Mississippi River Forecast Center (LMRFC). LMRFC is responsible for disseminating radar and rain gauge data from that region, neighboring River Forecast Center (RFC)'s were not able to completely fill in the gap. The lack of radar-based data made it difficult to validate Katrina's rainfall. This illustrates an instance where satellite-based data, Fig. 1 (right) with no missing, would prove highly valuable due to the absence of other sources of rainfall information.

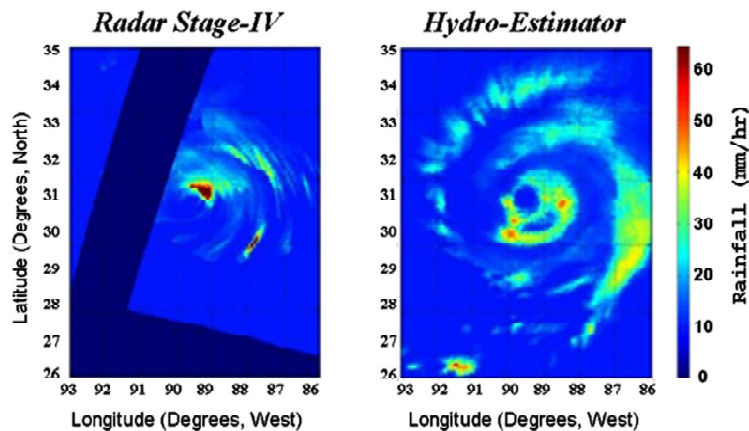


Figure 1: Rainfall Maps of Hurricane Katrina After Making Landfall on 08/29/2005 from Radar (Left) with Missing Data and from Satellite (Right) with no Missing Data

However, the cloud property information from satellite-based observations is not always directly related to the location and intensity of precipitation at the ground surface. Indirect estimation of rainfall distribution and intensity is the disadvantage of using remotely sensed cloud information. The most common satellite-based instruments that are used to estimate precipitation are geostationary Infrared (IR) and polar orbiting Microwave (MW) sensors. As the result of numerous research efforts in the last few decades, there are now several

satellite-based algorithms running operationally and semi-operationally, retrieving rainfall from cloud IR and/or MW information at various spatial and time scales.

The present study focuses on evaluating several satellite-based rainfall products for severe hurricanes because it is very important to understand the expected error characteristics of satellite-based rainfall retrievals, particularly for severe storms. Validation of satellite-based rainfall products should quantify their accuracy; give users information on the expected errors in the estimates; help algorithm developers understand the strengths and weaknesses of the products (including which aspects are in greatest need of improvement); monitor the performance of existing algorithms; and assist with evaluating algorithm upgrades. The rainfall products examined in this study are from the operational National Oceanic and Atmospheric Administration (NOAA) National Environmental Satellite, Data, and Information Service (NESDIS) Hydro-Estimator (HE) [5], the experimental NOAA/NESDIS Geostationary Operational Environmental Satellites (GOES) Multi Spectral Rainfall Algorithm (GMSRA) [6], the University of California at Irvine Precipitation Estimation from Remotely Sensing Information using an Artificial Neural Network system with Cloud Classification Scheme (PERSIANN-CCS) [7], and the National Aeronautics and Space Administration (NASA) Tropical Rainfall Measuring Mission (TRMM) Multi-satellite Precipitation Analysis (TMPA) 3B42RT product (TMPA-3B42) [8, 9]. The study cases are five major land-falling hurricanes: Charley (Category-4), Frances (Category-4), and Jeanne (Category-3) from 2004 and Rita (Category-5) and Wilma (Category-5) from 2005, which all created devastating losses of human life and economic damage.

Numerous efforts to evaluate the performance of satellite rainfall algorithms have been undertaken, but generally for regional, seasonal and climate impacts, for space and time variability, or at the resolution coarser than hourly 4-km that used in this study to validate strong hurricanes. These efforts include: evaluation of a rapid-update satellite-based precipitation considering space and time scales [10]; verification of precipitation in weather systems for determination of systematic errors [11]; comparison of satellite-based real time precipitation estimates against numerical model outputs [12]; and validation of NESDIS rainfall products for tropical potential (TRaP) forecasts for Australian tropical cyclones [13]; evaluation of TMPA products for hurricanes [14]; validation of the Global Precipitation Climatology Project (GPCP) rainfall fields at monthly 2.5 degrees [15]; and the ongoing real-time validation of daily rainfall at 0.25 degrees scale under the auspices of the International Precipitation Working Group (IPWG) for the U.S. and Mexico http://cics.umd.edu/~johnj/us_web.html and over Australia and Western Europe (<http://www.isac.cnr.it/~ipwg/validation.html>). Real-time statistical validation for several algorithms at 4-km resolution but at 6-hourly and daily time scales over the continental United States is being performed at the NOAA-NESDIS Center for SaTellite Applications and Research (STAR) at <http://www.star.nesdis.noaa.gov/smcd/emb/ff/aboutProductValidation.php>.

1.1 Selected Satellite-Based Rainfall Retrieval Algorithms

NEXRAD Stage-IV: NEXRAD Stage-IV product (a CONTinental United States (CONUS)-wide mosaic of the Stage-III fields described in [16]), at hourly 4 km × 4 km resolutions, is used as

a reference data source in the present study. Because, in comparison with rain-gauge observations, radar stage-IV rainfall data is a bias-corrected product that has been calibrated in near-real time using rain gauges. Although radar data have significant limitations, particularly in regions of significant topographic relief [17-18] and very large water bodies (e.g., seas and oceans) they do provide a source of area-averaged rainfall that results in a more appropriate comparison with satellite estimates than point values from rain gauges. This is particularly true for the validation region of this paper (the southeastern United States), where the radar network is relatively dense and the topography is generally flat enough to preclude significant beam block effects. Besides the above-mentioned reasons for selecting radar stage-IV rainfall as the true values, a rain gauge observation encounters some uncertainties associated with the error sources due to high moving speed, oblique angles, and heavy amounts of rainfall from hurricanes that radar does not.

Hydro-Estimator (HE) Algorithm: The Hydro-Estimator [5] was developed by Clay Davenport at NESDIS/STAR. It has been the operational satellite-based rainfall algorithm at NESDIS since fall 2002, and has been available since the spring of 2004 on the Advanced Weather Interactive Processing System (AWIPS), which is used by National Weather Service field forecasters. Rainfall fields from the HE are produced at 4-km spatial resolution every 15 minutes using GOES-E and -W observations, over the CONUS, with hourly, 3-hourly, and 6-hourly totals updated every 15 minutes and 24-hourly totals updated at 12:00 UTC. HE products can be accessed at <http://www.star.nesdis.noaa.gov/smcd/emb/ff/HydroEst.php>. The HE was developed as an improvement to the original Auto-Estimator (AE) algorithm developed by [19]; specifically, to eliminate the tendency of the AE to incorrectly assign heavy rainfall to cirrus clouds and thus greatly exaggerates the spatial extent of heavy rainfall [20] – a weakness that required the use of radar to screen out false raining pixels [21]. HE identifies raining clouds based on both pixel Brightness Temperature (BT) in GOES infrared (channel-4, 10.7 μm wavelength) and its value relative to its surroundings – pixels that are colder or warmer than their neighbors are presumed to be regions with updrafts and rainfall or regions with no updrafts and no rainfall, respectively. Rainfall rate is estimated as a function of pixel BT, its surrounding values, precipitable water, relative humidity, convective equilibrium level, and lower-tropospheric winds interfaced with terrain to diagnose regions of terrain-induced updrafts and downdrafts.

GMSRA: The experimental GMSRA uses combined information from visible (0.65 μm), near-infrared (3.9 μm), infrared-Water Vapor (WV; 6.7 μm), and thermal-infrared (10.7 μm) GOES measurements to produce high-resolution rainfall product at hourly 4 km \times 4 km resolutions over North America. For daytime rainfall, the first step consists of identifying optically thick clouds having a visible reflectance greater than 0.40. Non-precipitating cirrus is also screened empirically during the daytime and nighttime using a gradient temperature based on the 10.7- μm channel; in addition negative Brightness Temperature Differences (BTD) between the IR and WV channels, (IR-WV; 10.7 μm – 6.7 μm) correspond well with rainfall areas for very deep convective cores [22] and are further used to screen out cirrus clouds. Meanwhile, warmer clouds that are producing rainfall are identified during the daytime by deriving the effective radius of cloud particles near their tops from the reflected solar irradiance

at $3.9 \mu\text{m}$ – larger particles are associated with rainfall at higher brightness temperatures than would be otherwise considered. For each pixel that is classified as raining, the associated instantaneous rain rate is computed using a pre-calibrated probability of rain and mean rain rate for cloud top brightness temperature ($11 \mu\text{m}$) groups of 10 K.

PERSIANN-CCS: PERSIANN is based on Artificial Neural Network (ANN) systems for classification and approximation procedures to compute an estimate of rainfall rate at each $0.25^\circ \times 0.25^\circ$ pixel using cloud-top infrared brightness temperature provided by geostationary satellites. An adaptive training feature facilitates updating of the network parameters whenever independent estimates of rainfall are available. PERSIANN [7] was based on only geostationary IR but later extended [23] to include the use of both infrared and daytime visible imagery as well. The PERSIANN algorithm used here is based on the GOES-IR imagery only, while the TRMM Microwave Imager (TMI) 2A12 product provided by the TRMM satellite is used for regular updating of the network parameters [24]. The PERSIANN system uses grid infrared images of global geosynchronous satellites (GOES-East, GOES-West, GMS-5, Metsat-6, and Metsat-7) provided by National Climatic Data Center (NCDC), and TRMM-TMI instantaneous rain product (2A12) of NASA [25] to produce rainfall for coverage of 50°S to 50°N globally. The PERSIANN-CCS algorithm [26] that is evaluated in this paper is combination of PERSIANN and a Cloud Classification Scheme (CCS), using an artificial neural network and cloud top IR from GOES channel 4 and produces rainfall estimates at $4 \text{ km} \times 4 \text{ km}$ resolution.

TMPA-3B42: TMPA-3B42 algorithm estimates rainfall rate from combination of TRMM Microwave (TMI) merged with high quality (HQ) multi-sources MW from low and polar orbiting and IR from geostationary satellites [27]. TMPA-3B42 products are at 3-hourly time scale and a 0.25° by 0.25° spatial resolution at latitude and longitude directions in a global belt extending from 50 degrees south to 50 degrees north latitude. The 3B42 product, a combination of the TRMM real-time merged passive microwave and microwave-calibrated infrared-based estimates, produced in four stages: (1) microwave estimates precipitation are calibrated against ground-based observations; (2) infrared precipitation estimates are created using the calibrated microwave precipitation; (3) microwave and IR estimates are combined; and (4) rescaling to different time scales. Each precipitation field is best interpreted as the precipitation rate effective at the nominal observation time. TMPA data has been disaggregated in order to be able to be compared with other algorithms at 4 km resolution. The main objective of evaluating TMPA-3B42 is to test if this algorithm is capable of producing rainfall data that can be used as a reference data for validation of behaviors of satellite-based algorithms on capturing correct information from hurricanes before making landfall.

1.2 Study Cases and Selected Hurricanes

To evaluate the quality of four satellite-based rainfall products for Category-4 or -5 hurricanes, two study sites selected: (1) one over Florida (Fig. 1-left), with the coordinates of: $80\text{-}84$ degrees-west longitude and $25\text{-}30$ degrees north latitude, where hurricanes Charley, Frances, Jeanne, and Wilma landed over; and (1) one over Louisiana (Fig. 2-right), with the coordinates of $87\text{-}97$ degrees-west longitude and $25\text{-}35$ degrees north latitude, where hurricane Rita landed over.

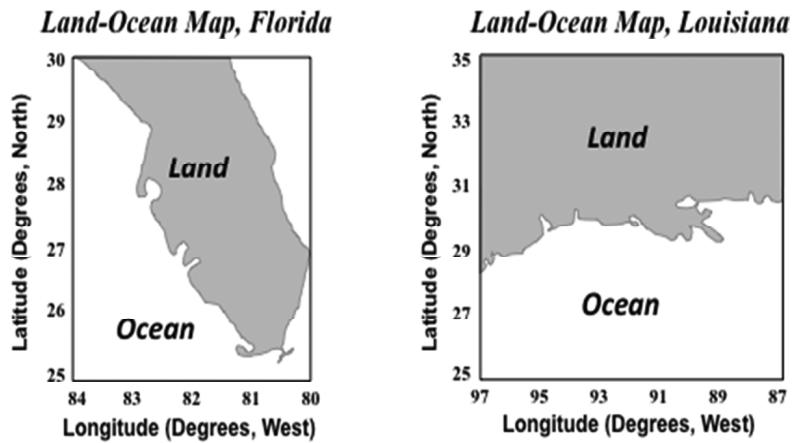


Figure 2: Study Areas, over Florida (Left), Landfall of Hurricanes Charley, Frances, Jeanne, and Wilma; and over Louisiana (Right), Landfall of Hurricane Rita

The selected five strong hurricanes, their detailed information can be found at: <http://www.nhc.noaa.gov/pastall.shtml#tcr>, are:

Hurricane Charley (Category-4): Charley formed on August 9th 2004 as a tropical depression and slowly strengthened and reached to strength of a hurricane on August 11th, as it turned to a more northerly track from Jamaica. Charley rapidly intensified with surface wind speed of 145 mph before becoming a powerful category-4 hurricane. Hurricane Charley made landfall along the west coast of Florida on August 13th with surface wind of 111 mph. Charley maintained hurricane strength as it moved across the Florida Peninsula until it became category-1 as it reached to the east coast and re-emerged over Atlantic waters with wind speed of about 86 mph. Total rainfall from Charley was about 1-3 inches in many locations along the East Coast. At least 16 people were killed, over 2 million customers lost power as Charley moved across Florida, and the total economic loss was over 10 billion US dollars.

Hurricane Frances (Category-4): Hurricane Frances formed in August but made landfall on September 5th 2004 in Florida. On September 1st hurricane Frances moved towards the southeastern Bahamas as a Category-4 hurricane, with estimated surface wind of 140 mph and gradually moved west-northwestward across the central Bahamas. The eye of Frances finally made landfall the first time on September 5th near Sewall's Point, Florida with maximum wind speed of 105 mph, and for the second time on September 6th near St. Marks in Florida with wind speed of 65 mph. Frances started to weaken to a tropical depression as moved north and into the Northeast. Over the next several days, very heavy rain exceeding 15 inches fell in some locations that resulted in very extensive flooding and damage, particularly from Georgia to New York.

Hurricane Jeanne (Category-3): Hurricane Jeanne formed as a tropical wave on September 14, 2004 then reached hurricane with Category-2 strength on September 18 and Category-3 strength on the 25th. As a Category-3 hurricane, Jeanne continued westward and made landfall

at midnight on September 26 over Stuart in Florida, the location where hurricane Frances made landfall 20 days earlier, with wind speeds of 120 mph. Hurricane Jeanne, after making landfall, moved northward and gradually weakened to a tropical storm and then tracked across Georgia and Carolinas until it re-emerged over the Atlantic east of New Jersey on September 29th. Heavy rain fell from Jeanne along its track over land and the resulting flooding caused over 3000 lost lives, though only in Haiti.

Hurricane Rita (Category-5): Hurricane Rita developed on September 18, 2005 from a tropical depression and became a Category-2 hurricane by September 20. Rita tracked westward into the Gulf of Mexico and intensified rapidly that became Category-5 hurricane with wind speeds of 165 mph by the afternoon of September 21. Hurricane Rita continued to intensify as a Category-5 and reached top wind speeds of 180 mph over the central Gulf of Mexico but made landfall as a Category-3 hurricane on September 23 in southwestern Louisiana. Hurricane Rita was a devastating storm, with high speed wind, heavy rain, and tornadoes that caused extensive damages and fatalities from eastern Texas to Alabama. Significant amounts of rain from Rita also produced flooding in parts of the Florida Keys as well.

Hurricane Wilma (Category-5): Wilma was the third Category-5 hurricane in 2005 Hurricane Season that reached top wind speeds of 185 mph on October 19. Wilma weakened on the 21st of October and then strengthened again causing hurricane force as a Category-4 hurricane during the few hours before making landfall in Mexico on October 22nd. Wilma made another landfall on October 24th in southwestern Florida as a Category-3 hurricane with top wind speeds of 120 mph. Wilma was the most intense recorded Atlantic tropical cyclone and caused extensive damages on the Yucatán Peninsula of Mexico, Cuba, and Florida due to its slow-moving and multiple landfalls. Wilma, ranked among the top costliest hurricanes ever recorded in the Atlantic, was responsible for at least 63 deaths and over \$29.1 billion (\$20.6 billion in the U.S.) estimated damages.

2. METHODOLOGY

The validation strategy in the present study is statistical analysis and comparisons between rainfall estimates from the satellite-based Hydro-Estimator, GMSRA, PERSIANN-CCS, and TMPA-3B42 with NEXRAD Stage-IV fields. Despite the spatial limitation of radar coverage, NEXRAD Stage-IV was selected as benchmark rainfall values because radar rainfall represents areal averages and is thus a more appropriate reference for validation of areal-based satellite estimates than point-based rain gauge observations. Furthermore, rain gauges are subject to under-catch during instances of very intense rainfall and strong winds, both conditions of which are present during strong hurricanes. The validation strategy is summarized as follows:

- Evaluate detailed spatial distributions and rainfall patterns by detailed comparison of hourly and cumulative rainfall images. Cumulative rainfall in this study is total rainfall from hurricane for several numbers of hours, up to 24 hours, after making landfall.
- Evaluate rainfall-intensity distributions by comparison of rainfall frequency values and changes using hourly-based histograms,

- Evaluate time variability and distribution of satellite-based rainfall intensity against Stage-IV, using 3-hourly time series analysis for the time period that each hurricane after making landfall to examine the behavior of these algorithms to capture rainfall changes over time.
- Comparison of hourly and cumulative pixel-to-pixel rainfall amounts by construction of scatterplots and calculation of summary statistics.

3. RESULTS AND DISCUSSION

This validation study consisted of evaluations the performances of four satellite-based rainfall retrieval algorithms (HE, GMSRA, PERSIANN-CCS, and TMPA-3B42) for five very strong hurricanes: Charley, Frances, and Jeanne (in 2004) and Rita and Wilma (in 2005) after making landfall, which is described as following:

3.1 Evaluation of Spatial Distributions and Rainfall Pattern

The performance of the selected algorithms, at capturing rainfall distribution, size, and spatial patterns of 5 category-4 and -5 strength hurricanes, has been evaluated by comparing rainfall images of each algorithm with NEXRAD Stage-IV rainfall maps on an hourly basis. Each algorithm behaves differently for each hurricane even from one hour to the next hour. For brevity, the comparison images included in this paper are only for one hour – the hour that the algorithm gives the most common behavior in comparison with Stage-IV – and the total rainfall during the time that the hurricane was moving over land after making landfall. In Figs. 3 to 7, the top images are hourly rainfall and bottom images are cumulative rainfall maps for the selected five hurricanes.

- ***Hurricane Charley (17 – 24 UTC, August 13, 2004, Florida):*** The evaluation of the rainfall amounts and distributions from the four satellite-based rainfall retrieval algorithms for hurricane Charley is shown by comparing the performances of three of the selected algorithms on capturing rainfall with Stage-IV, after Charley landed in Florida on August 13th, in Fig. 3. The top images are the 1-hour rainfall maps for 21-22 UTC and the bottom images are accumulated rainfall for the hours of 18-24 UTC. The hour of 21-22 UTC has been selected because it exhibits typical rainfall patterns for most of the hours after Charley landed. PERSIANN-CCS rainfall data is not readable for the selected hours after Charley made landfall. According to Fig. 3, the HE and TMPA are in a much better agreement than GMSRA at capturing the locations, distributions, and patterns of rainfall in comparison with NEXRAD Stage-IV rainfall information. The GMSRA is not successful at capturing the hurricane eye and pattern, particularly, at the hourly time scale. The image of total rainfall from GMSRA shows that the heaviest rainfall is misplaced northward in comparison with Stage-IV as well as the HE and TMPA total rainfall maps. Figure 3 also demonstrates that all of the selected satellite-based algorithms underestimated rainfall amount, particularly for heavier rainfall, in comparison with Stage-IV – especially the GMSRA, which gives very low rainfall amounts over too wide an area.

EVALUATION OF REMOTELY SENSED RAINFALL ALGORITHMS FOR STRONG HURRICANES

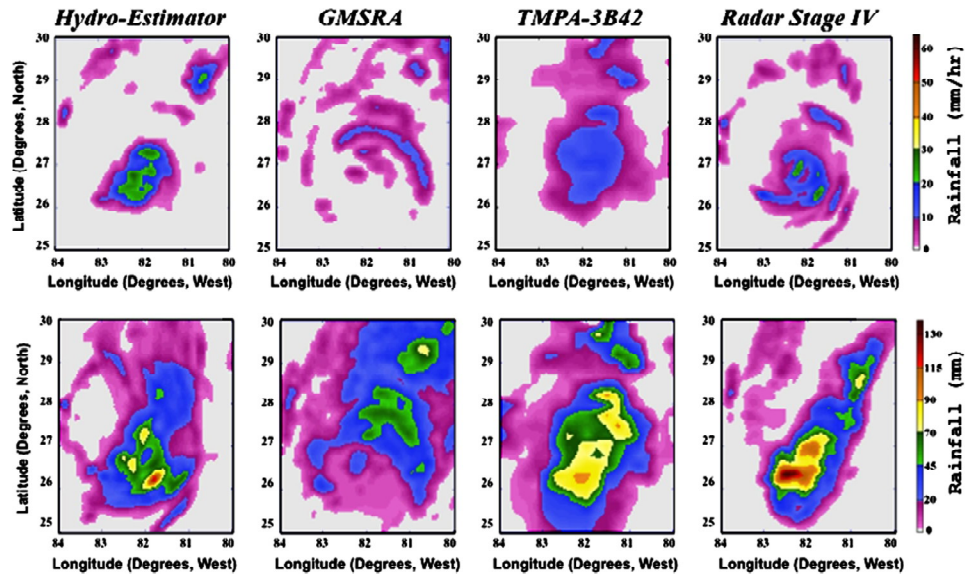


Figure 3: Comparison of Rainfall Estimates from HE, GMSRA, and TMPA with Stage-IV, for Hurricane Charley, for One Hour Starting at 21 UTC (Top) and the Accumulated Rainfall for the Hours of 17-24 UTC (Bottom) on August 13, 2004

- Hurricane Frances, 00-24 UTC, September 05, 2004 in Florida:** To evaluate the amounts and distributions of rainfall from hurricane Frances after making landfall, the rainfall maps of the selected four algorithms are compared in Fig. 4. The top images of Fig. 4 are rainfall maps at the hour of 15-16 UTC and the bottom images are the cumulative rainfall maps for the 24 hours of 00-24 UTC after Frances made landfall in Florida. According to Fig. 4, the images of hourly and total rainfall both show that rainfall distributions from all algorithms, except for the GMSRA, are reasonably similar to the Stage-IV rainfall distribution but with underestimated rainfall intensity. The GMSRA cannot capture the heaviest rain near the eye of the hurricane. The HE produces the largest areas of moderate to heavy rainfall and with the rainfall patterns very similar to Stage-IV in comparison with rainfall estimates from the other selected algorithms for evaluation in this study. The HE and PERSIANN-CCS distributions are very similar to each other at hourly scales. The GMSRA gives the lowest intensity overall, while the highest TMPA rainfall amounts are lower than PERSIANN-CCS at hourly scales but the broader distribution of the TMPA rainfall results in higher totals on the cumulative rainfall images. The cumulative rainfall maps, bottom images, demonstrate that all algorithms produce similar pattern and location of rainfall but a little bit larger and with small longitudinal shift in comparison with Stage-IV rainfall maps. All algorithms produce underestimated rainfall, particularly GMSRA, in comparison with Stage-IV rainfall magnitudes. GMSRA is also the poorest algorithm to capture rainfall distribution in comparison to other algorithms.

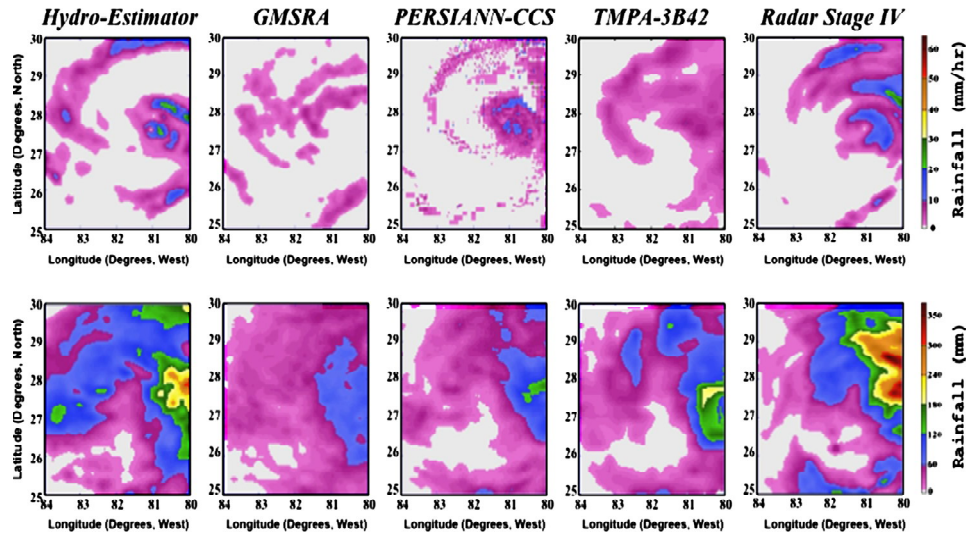


Figure 4: Comparison of Rainfall Estimates from HE, GMSRA, PERSIANN-CCS, and TMPA with Stage-IV, for Hurricane Frances, for One Hour of 15-16 UTC (Top) and the Accumulated Rainfall for the Hours of 00-24 UTC (Bottom) on 09/05/2004

- Hurricane Jeanne, 00-24 UTC, September 26, 2004 in Florida:* Images of satellite-based rainfall distributions for hurricane Jeanne after landing in Florida on September 26 are shown for 1-hour of 06-07 UTC (top images), and for accumulations (bottom

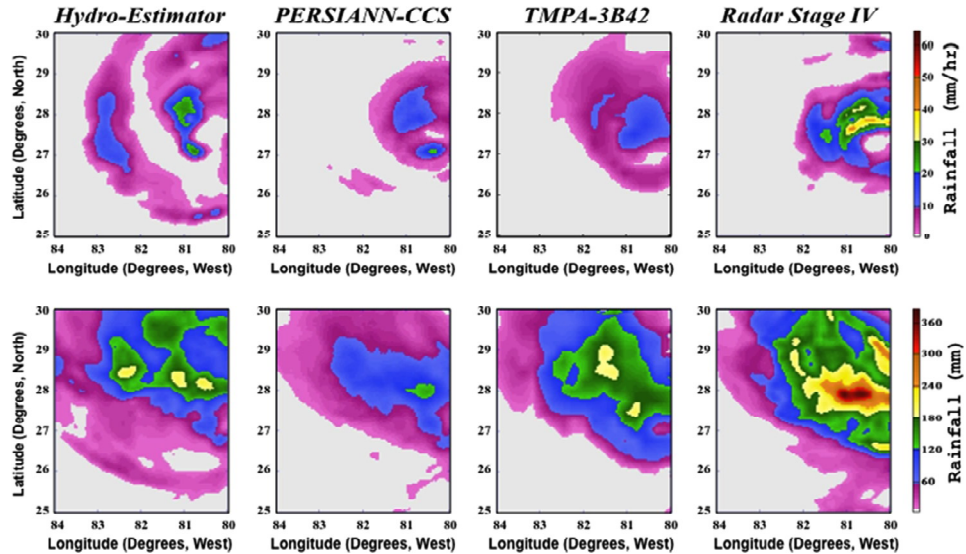


Figure 5: Comparison of Rainfall Estimates from HE, PERSIANN-CCS, and TMPA with Stage-IV for Hurricane Jeanne, for One Hour of 06-07 UTC (Top) and the Accumulated Rainfall for Hours of 00-24 UTC (Bottom) on 09/26/2004

EVALUATION OF REMOTELY SENSED RAINFALL ALGORITHMS FOR STRONG HURRICANES

images) for 00-24 UTC in Fig. 5. GMSRA data is not readable for this case. According to the Fig. 5 images, almost all of the satellite-based algorithms produce rainfall at approximately the same locations as Stage-IV but with underestimated amounts, similar to their behaviors for hurricane Frances (Figs 4). The HE produces rain over the largest area while PERSIANN-CCS has the smallest rainfall coverage for hourly data in comparison with Stage-IV. Also, the rainfall intensity from PERSIANN-CCS is much less than the HE and TMPA rainfall values.

- Hurricane Rita, 00-18 UTC, September 24, 2005 in Louisiana: Fig. 6 shows the satellite-based rainfall distributions in comparison with Stage-IV fields for hurricane Rita after making landfall in Louisiana on September 24, 2005. Images of hourly rainfall for hour of 03-04 UTC (top) and cumulative rainfall for hours of 00-18 UTC (bottom) from all satellite-based algorithms show the same locations for the heaviest rainfall cells. The rainfall patterns for all algorithms' products are similar, particularly for heavier rainfall amounts. The HE and GMSRA have the largest areal coverage of rainfall with more intense heavier rainfall for the HE. The satellite-based algorithms in general underestimated rainfall intensities, except for the HE. PERSIANN-CCS produces the smallest amounts of rainfall, both at hourly basis and total values after making landfall, in comparison with other algorithms. It should be noted that the GMSRA rainfall intensity for Rita is not as small as for the other hurricanes.

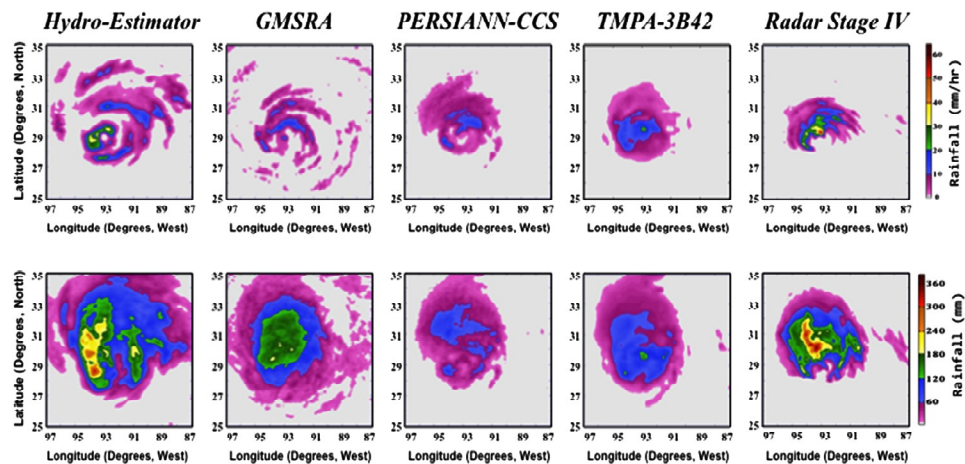


Figure 6: Comparison of Images of Rainfall from HE, GMSRA, PERSIANN-CCS, and TMPA with Stage-IV for Hurricane Rita, for One Hour of 03-04 UTC (Top), and the Accumulated Rainfall (Bottom) for Hours of 00-18 UTC on 09/24/2005

- **Hurricane Wilma, 12i18 UTC on October 24, 2005 in Florida:** A comparison between satellite-based against Stage-IV rainfall images for hurricane Wilma is shown in Fig. 7. At hourly scales (12-13 UTC, top), rainfall patterns from the HE and PERSIANN-CCS are more similar to the Stage-IV rain pattern compared to the other algorithms. However, distributions of rainfall intensities from all algorithms are somewhat different from

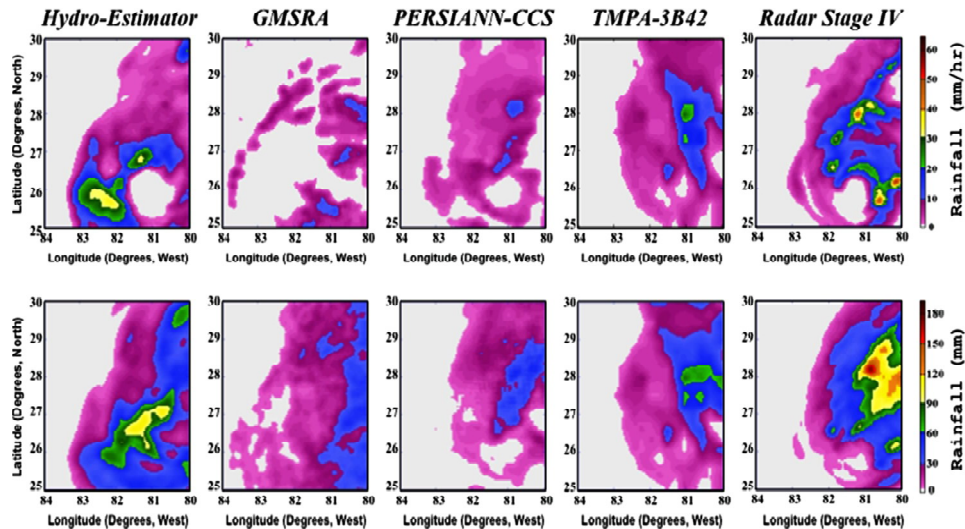


Figure 7: Comparison of the Images of Rainfall from the HE, GMSRA, PERSIANN-CCS, and TMPA with Stage-IV for Hurricane Wilma, for One Hour of 12-13 UTC (Top) and Accumulated Rainfall for Hours of 12-18 UTC (Bottom) on 10/24/2005

each other. The HE produces higher values over a wider area in comparison with other algorithms, particularly for the western flank of the hurricane where Stage-IV does not give large rainfall values. GMSRA and PERSIANN could not capture heavy rainfall parts at hourly time scale and total, both. According to accumulated rainfall images (bottom) for 12-18 UTC, the rainfall pattern from the HE is very different from rainfall patterns of other algorithms and Stage-IV. PERSIANN-CCS, TMPA, and the GMSRA significantly underestimated rainfall intensities with compare to Stage-IV at time scale of hourly and 6-hourly total rainfall, both.

3.2 Evaluation of Rainfall Intensity Distribution

To evaluate rainfall-intensity distributions regardless of their spatial characteristics, rainfall histograms from the satellite algorithms are compared with Stage-IV rainfall histograms at hourly 4 km resolutions in Figure 8. To make these comparisons more realistic only the hours that all of the algorithms have rainfall products have been selected. The GMSRA histogram, which gives a very different rainfall intensity distribution from the other algorithms, shows that although GMSRA generally underestimates rainfall values, the frequency of pixels with rainfall smaller than 2 mm/hr is much less than the frequency of similar pixels from other algorithms. And, the number of pixels with rainfall intensity between 16 and 20 mm/hr are greater than the number of similar pixels from the other algorithms. The HE histogram exhibits the greatest number of pixels with rainfall intensity smaller than 16 mm/hr and greater than 20 mm/hr. The trend of frequency changes of HE rainfall is very similar to the one from Stage-IV rainfall for intensities greater than 4 mm/hr. According to these histograms, after HE, TMPA covers the next-largest areas with rainfall intensities smaller than 10 mm/hr. The frequency

EVALUATION OF REMOTELY SENSED RAINFALL ALGORITHMS FOR STRONG HURRICANES

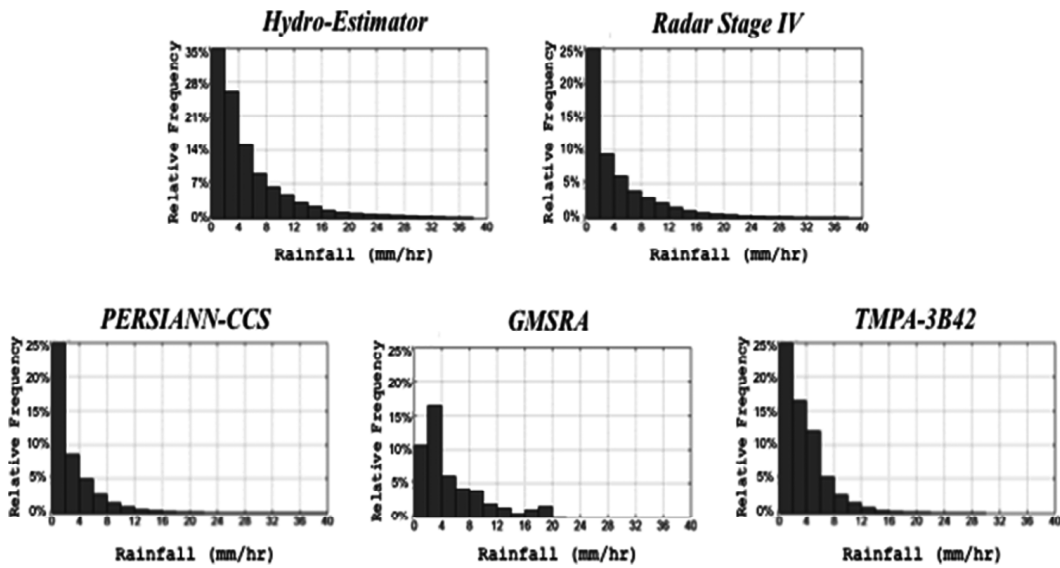


Figure 8: Comparison between Distributions of Rainfall Intensities from Four Algorithms of HE, GMSRA, PERSIANN-CCS, and TMPA with Stage-IV

trend of rainfall frequencies from PERSIANN-CCS is similar to the Stage-IV rainfall trend but with sharper gradient that gives much fewer pixels for greater rainfall amounts. In general, the maximum Stage-IV and HE rainfall values exceed 35 mm/hr but the maximum rainfalls from other algorithms are smaller than 25 mm/hr.

3.3 Evaluation of Time Variability of Rainfall Intensity Distribution

The time variability of rainfall intensity from satellite-based algorithms has been investigated in comparison with the Stage-IV time series of rainfall at 3-hourly time scales for up to the first 24 hours after each hurricane made landfall. Figure 9 compares the time series of 3-hourly rainfall (average rainfall every 3 hours in hourly basis) from each satellite-based algorithm (solid lines) with corresponding time series from Stage-IV (dashed lines). According to Fig. 9, the HE rainfall time variability, in general, does not match the Stage-IV time series except for brief periods, particularly for hurricane Charley with overestimated rainfall and for hurricane Jeanne with underestimated rainfall. The GMSRA time variability of rainfall matches with Stage-IV rainfall changes well for hurricane Charley and for hurricane Frances after 3 UTC. PERSIANN-CCS rainfall time changes match the time variability of Stage-IV rainfall for the most part of the day and almost for all hurricanes, particularly hurricanes Rita and Wilma. However, PERSIANN-CCS greatly underestimated rainfall for hurricanes Frances and Jeanne. The time variability of rainfall from TMPA does not match with Stage-IV time series for any of the hurricanes. TMPA in general produces over estimated rainfall, particularly for hurricanes Charley and Wilma.

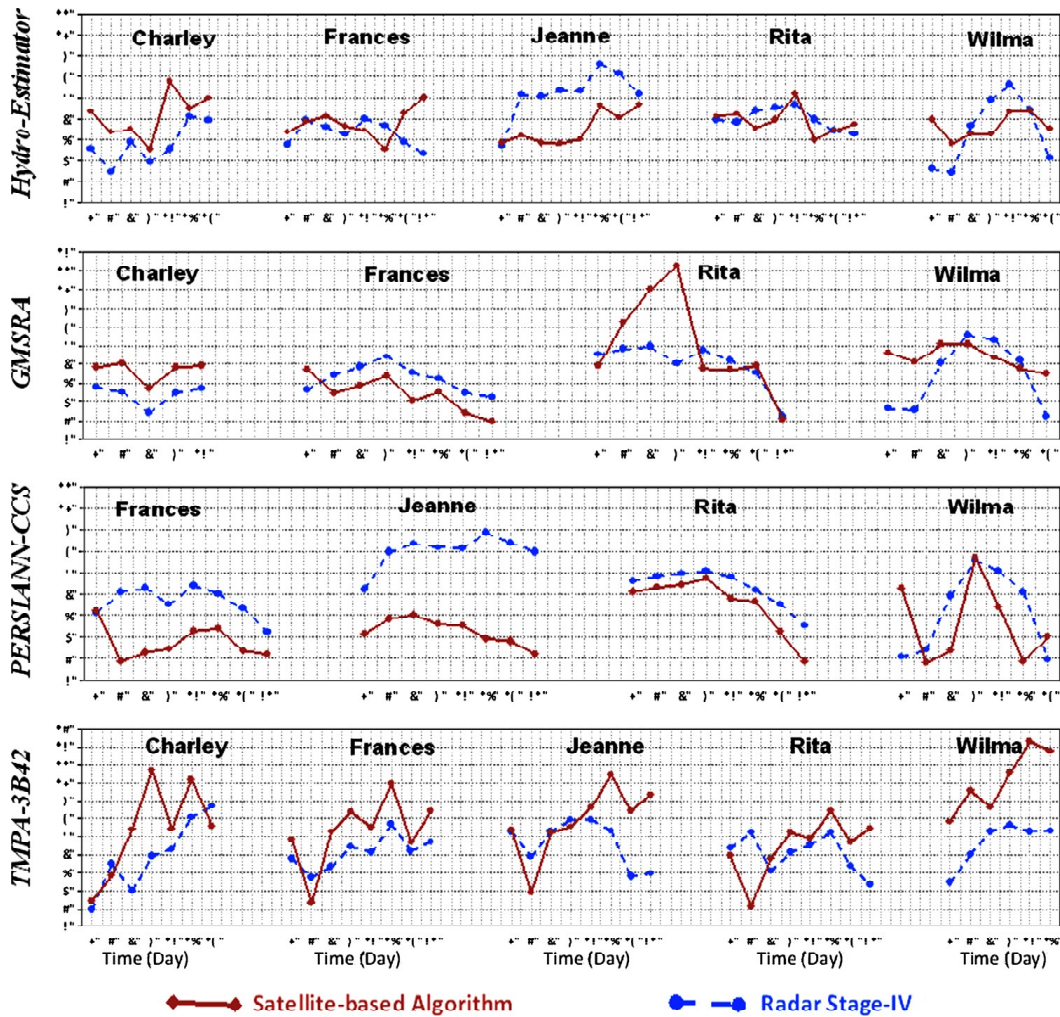


Figure 9: Comparing Time Series of 3-Hourly Rainfall from HE, GMSRA, PERSIANN-CCS, and TMPA Algorithms (Dashed Blue) with the One from Stage-IV (Solid Red) for 5 Selected Hurricanes

3.4 Evaluation of Pixel-based Total Rainfall Distribution

Comparison of cumulative pixel-to-pixel rainfall amounts from satellite-based algorithms with the Stage-IV for the selected 5 hurricanes, at 4-km spatial resolution, has been performed by construction of scatterplots and calculation of summary statistics, such as coefficient of determination (R-square), Root Mean Square Error (RMSE), and bias to investigate the accuracy of spatial and temporal variations in rainfall intensity for these satellite-based rainfall estimates during severe hurricanes. Figure 10 and Table 1 show respectively the scatterplots and statistical parameters of rainfall from satellite-based algorithms versus Stage-IV only for the pixels that both indicate non-zero rainfall amounts. According to the scatterplots shown in Figure 10 and

EVALUATION OF REMOTELY SENSED RAINFALL ALGORITHMS FOR STRONG HURRICANES.

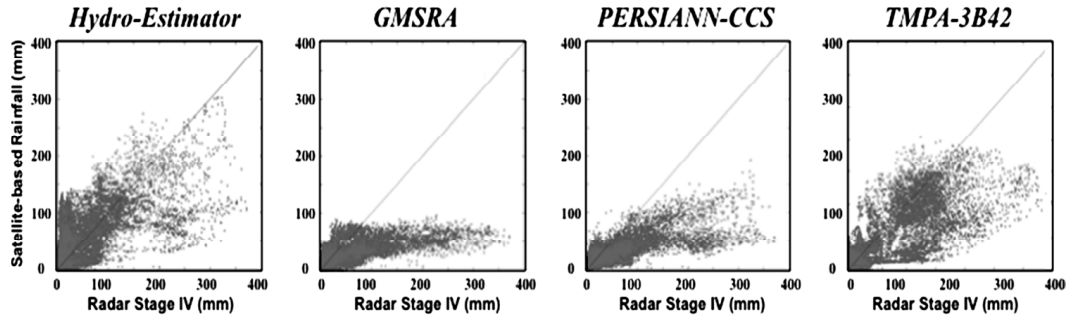


Figure 10: Comparing Pixel-to-Pixel Satellite-Based Accumulated Rainfall for the Time that Each of the Selected 5 Hurricanes was Moving Over Land After Making Landfall vs. Corresponding Pixels from Stage-IV

Table 1, PERSIANN-CCS vs. Stage-IV gives a narrower distribution with highest correlation but with very large RMSE and the greatest bias because of underestimation of this algorithm. The GMSRA vs. Stage-IV is also giving a narrow distribution with the smallest correlation, the greatest RMSE and high absolute bias value. The distributions of both HE and TMPA vs. Stage-IV are wide. TMPA rainfall is more highly correlated with Stage-IV than HE rainfall with smaller RMSE and greater bias in comparison with RMSE and bias for HE vs. Stage-IV.

Table 1
Comparison of Statistics of Pixel-to-Pixel Accumulated Rainfall from Satellite-based Algorithms vs. Stage-IV for the Selected 5 Hurricanes

	<i>Hydro-Estimator</i> vs. <i>Stage-IV</i>	<i>GMSRA</i> vs. <i>Stage-IV</i>	<i>PERSIANN-CCS</i> vs. <i>Stage-IV</i>	<i>TMPA-3B42</i> vs. <i>Stage-IV</i>
R²	0.62	0.61	0.76	0.74
RMSE (mm)	52.77	63.51	58.29	49.18
Bias (mm)	5.43	-28.27	-29.72	-18.29

4. CONCLUSIONS AND SUMMARY

The performance of five satellite-based rainfall algorithms (Hydro-Estimator and GMSRA from NESDIS, PERSIANN-CCS from CHRS (Center for Hydrometeorology & Remote Sensing), and TMPA-3B42 from NASA) are evaluated against NEXRAD Stage-IV, which is a rain gauge-adjusted radar-based field, for five strong hurricanes from 2004 (Charley, Frances, and Jeanne) and 2005 (Rita and Wilma) after making landfall. The hourly and accumulated rainfall maps and statistical analysis of data distributions, time series, and scatterplots support the following conclusions:

The magnitude and trend of rainfall intensity from the Hydro-Estimator agree best with Stage-IV measurements but still have different spatial distribution and coverage than Stage-IV for the most of the hurricanes. The HE produces the largest spatial coverage for all rainfall values in comparison with Stage-IV for most storms. The HE also exhibits larger spatial errors

particularly for the pixels with greater amounts of rainfall, depicting large amounts of rainfall for some of the pixels at which Stage-IV produces little or no rainfall. Maximum HE rainfall intensity, which exceeds 35 mm/hr for most hours, is smaller than the Stage-IV maximum for most hours. The time variability of HE rainfall, in general, does not match with the Stage-IV time series except for a few brief periods. Pixel-to-pixel comparison of total rainfall from HE vs. Stage-IV at 4 km resolution demonstrates a wide distribution with not a very high correlation but with the least bias.

The GMSRA rainfall maps reveal that behavior of this algorithm varies for different hurricanes with respect to Stage-IV but in general significantly underestimates rainfall with differences in coverage and distribution compared to Stage-IV. The GMSRA produces large areas of light rainfall that generally do not appear in Stage-IV. This algorithm is not successful in capturing the hurricane eye, storm patterns, and the parts of hurricanes with greatest amount of rainfall, particularly at hourly time scales. The frequency distribution analysis demonstrates that although this algorithm in general covers wider areas for low rainfall values, the number pixels with very low rainfall amounts (smaller than 2 mm/hr) are much less than the similar ones from other algorithms. Only for a small range of larger rain values (between 16 and 20 mm/hr) does the GMSRA produce a larger number of pixels in comparison with the number of similar pixels from Stage-IV and also other algorithms. Time series analysis indicates that GMSRA rainfall does not agree well with the trends of Stage-IV rainfall time variability for almost all storms, except for hurricane Charley and some part of the day for hurricane Frances. Pixel-to-pixel comparison of total rainfall at 4 km resolution from GMSRA vs. Stage-IV shows a narrow distribution with the lowest correlation and greatest RMSE.

PERSIANN-CCS underestimates rainfall intensity with respect to Stage-IV rainfall at hourly scales and also underestimates total volume for all hurricanes analyzed here, particularly Frances and Jeanne but the distribution of PERSIANN-CCS rainfall intensity changes match better with Stage-IV rainfall distribution than the ones from other algorithms. The total rainfall at 4 km resolution from PERSIANN-CCS vs. Stage-IV at pixel-based shows a narrower distribution than the HE and GMSRA with the highest correlation of the four satellite algorithms but very large RMSE and the greatest bias in comparison with the other algorithms. PERSIANN-CCS rainfall variations in time generally match with the time variability of Stage-IV rainfall, particularly for hurricanes Rita and Wilma. The distribution of rainfall frequencies from PERSIANN-CCS is similar to the Stage-IV rainfall trend but with a sharper gradient that gives much lower number of pixels for greater rainfall amounts.

The TMPA-3B42 rainfall distribution generally matches the with Stage-IV rainfall distribution better than the other algorithms with slight underestimation of rainfall amounts at hourly time scale and total rainfall scale. However, TMPA-3B42 also overestimated rainfall intensity for some hours particularly for hurricane Wilma. The frequency distribution of rainfall intensity from TMPA shows greater spatial coverage than the other algorithms for rainfall intensity smaller than 10 mm/hr. The time variability of rainfall from TMPA does not match the Stage-IV time series for any of the hurricanes. TMPA-3B42 behaves much better than other algorithms as far as capturing the correct location of storm as depicted by Stage-IV. According to the scatterplots in

EVALUATION OF REMOTELY SENSED RAINFALL ALGORITHMS FOR STRONG HURRICANES

Figure-10, total rainfall at 4 km resolution from TMPA-3B42 shows significant scatter compared to Stage-IV, but with very high correlation and high RMSE and bias.

In summary, comparison of the selected four remotely sensed rainfall retrieval algorithms with each other and against Stage-IV reveals that:

- The HE and TMPA-3B42 generally produce the most accurate measures of the relative rainfall amounts despite significant mis-location of pixels with large rainfall amounts or overestimation for pixels with very low rainfall values.
- The HE and GMSRA produce as the largest rainfall coverage whereas PERSIANN-CCS gives the smallest rainfall coverage for the most hourly data in comparison with Stage-IV.
- TMPA and PERSIANN-CCS generally produce rainfall patterns, which match more closely with Stage-IV than do the rainfall patterns from HE and GMSRA.
- PERSIANN_CCS, despite underestimating rainfall intensity, produces rainfall with the highest correlation against Stage-IV in comparison with the other algorithms' estimates
- The time and spatial variability of PERSIANN_CCS estimates also match better with the corresponding Stage-IV measurement changes in comparison with other algorithms.

Acknowledgements

This study was supported and monitored by National Oceanic and Atmospheric Administration (NOAA) under Grant NA06OAR4810162. The views, opinions, and findings contained in this report are those of the author(s) and should not be construed as an official National Oceanic and Atmospheric Administration or U.S. Government position, policy, or decision. The authors would like to acknowledge Dr. Arnold Gruber from NOAA-NESDIS for his valuable comments.

References

- [1] Kondragunta, C. R., and A. Gruber, (1997), Intercomparison of Spatial and Temporal Variability of Various Precipitation Estimates, *Advances in Space Research*, **19**(3), 457-460.
- [2] Masunaga H., T. S. L'ecuyer, and C. D. Kummerow, (2005), Variability in the Characteristics of Precipitation Systems in the Tropical Pacific, Part I: Spatial Structure, *Journal of Climate*, **18**, 823-840.
- [3] Gershunov A., and J. Michaelsen, (1996), Climatic-Scale Space-Time Variability of Tropical Precipitation, *Journal of Geophysical Research*, **101**(D21), pp. 26, 297-26, 307.
- [4] Singh K. K., and S. V. Singh, (1996), Space-Time Variation and Regionalization of Seasonal and Monthly Summer Monsoon Rainfall of the Sub-Himalayan Region and Gangetic Plains of India, *Climate Research*, **6**, 251-262.
- [5] Scofield R. A., and R. J. Kuligowski, (2003), Status and Outlook of Operational Satellite Precipitation Algorithms for Extreme-Precipitation Events, *Mon. Wea. Rev.*, **18**, 1037-1051.
- [6] Ba M. B., and A. Gruber, (2001), GOES Multispectral Rainfall Algorithm (GMSRA), *J. Appl. Meteor.*, **40**, 1500-1514.
- [7] Hsu K., X. Gao, S. Sorooshian, and H. V. Gupta, (1997), Precipitation Estimation from Remotely Sensed Information Using Artificial Neural Networks, *J. Appl. Meteorol.*, **36**, 1176-1190.

- [8] Huffman G. J., R. F. Adler, P. Arkin, A. Chang, R. Ferraro, A. Gruber, J. Janowiak, A. McNab, B. Rudolf, and U. Schneider, (1997), The Global Precipitation Climatology Project (GPCP) Combined Precipitation Data Set, *Bulletin of the American Meteorological Society*, **78**, 5-20.
- [9] Huffman G. J., Adler R. F., Bolvin D. T., Gu G., Nelkin E. J., Bowman K. P., Hong Y., Stocker E. F., and Wolff D. B., (2007), The TRMM Multi-Satellite Precipitation Analysis: Quasi-Global, Multi-Year, Combined-Sensor Precipitation Estimates at Fine Scale, *J. Hydrometeorol.*, **8**, 38-55.
- [10] Turk F. J., B.-J. Sohn, J.-J. Oh, E. E. Ebert, V. Levizzani, and E. A. Smith, (2009), Validating a Rapid-Update Satellite Precipitation Analysis Across Telescoping Space and Time Scales, *Meteorol. Atm. Phys.*, **105**, 99-108.
- [11] Ebert E. E., and J. L. McBride, (2000), Verification of Precipitation in Weather Systems: Determination of Systematic Errors, *J. Hydrology*, **239**, 179-202.
- [12] Ebert E. E., J. Janowiak, and C. Kidd, (2007), Comparison of Near Real Time Precipitation Estimates from Satellite Observations and Numerical Models, *Bull. Amer. Met. Soc.*, **88**, 47-64.
- [13] Ebert E. E., S. Kusselson, and M. Turk, (2005), Validation of NESDIS Operational Tropical Rainfall Potential (TRaP) Forecasts for Australian Tropical Cyclones, *Aust. Meteorol. Mag.*, **54**, 121-135.
- [14] Habib E., A. Henschke, and R. F. Adler, (2009), Evaluation of TMPA Satellite-Based Research and Real-Time Rainfall Estimates During Six Tropical-Related Heavy Rainfall Events Over Louisiana, USA, *Atmospheric Research*, **94**, 373-388.
- [15] Krajewski W. F., G. J. Ciach, J. R. McCollum, and C. Bacotiu, (2000), Initial Verification of the Global Precipitation Climatology Project Monthly Rainfall Over the United States, *J. Appl. Meteor.*, **39**, 1071-1086.
- [16] Fulton R. A., J. P. Breidenbach, D.-J. Seo, and D. A. Miller, (1998), The WSR-88D Rainfall Algorithm, *Wea. Forecasting*, **13**, 377-395.
- [17] Young C. B., B. R. Nelson, A. A. Bradley, J. A. Smith, C. D. Peters-Lidard, A. Kruger, and M. L. Baeck, (1999), An Evaluation of NEXRAD Precipitation Estimates in Complex Terrain, *J. Geophys. Res.*, **104**, 19691-19703.
- [18] Young C. B., A. A. Bradley, W. F. Krajewski, A. Kruger, and M. L. Morrissey, Evaluating NEXRAD Multisensor Precipitation Estimates for Operational Hydrologic Forecasting, *J. Hydrometeorol.*, **1**, 241-254.
- [19] Vicente, G.A., R.A. Scofield, and W. P. Menzel (1998); The operational GOES infrared rainfall estimation technique. *Bull. Amer. Meteor. Soc.*; Vol. 79, pp. 1883 – 1898
- [20] Rozumalski R. A., (2000), A Quantitative Assessment of the NESDIS Auto-Estimator, *Wea. Forecasting*, **15**, 397-415.
- [21] Scofield R. A., (2001), Comments on “A Quantitative Assessment of the NESDIS Auto-Estimator”, *Wea. Forecasting*; **16**, 277-278.
- [22] Inoue T., (1997a), Day-to-Night Cloudiness Change of Cloud Types Inferred from Split Window Aboard NOAA Polar-Orbiting Satellite, *J. Meteor. Soc. Japan*, **V(75)**, 59-66.
- [23] Hsu K., H. V. Gupta, and S. Sorooshian, (1999), A Neural Network for Estimating Physical Variables from Multi-Channel Remotely Sensed Imagery: Application to Rainfall estimation, *Water Resources Research*; **35**, 1605-1618.
- [24] Sorooshian S., K. Hsu, X. Gao, H. V. Gupta, B. Imam, and D. Braithwaite, (2000), Evaluation of PERSIANN System Satellite-Based Estimates of Tropical Rainfall, *Bulletin of American Meteorology Society*, **81**, 2035-2046.
- [25] Kummerow C. D., and Co-Authors, (2001), The Evolution of the Goddard Profiling Algorithm (GPROF) for Rainfall Estimation from Passive Microwave Sensors, *J. Appl. Meteorol.*, **40**, 1801-1820.
- [26] Hong Y., K. Hsu, S. Sorooshian, and X. Gao, (2004), Precipitation Estimation from Remotely Sensed Imagery Using an Artificial Neural Network Cloud Classification System, *J. of Appl. Meteo*, **43**, 1834-1852.
- [27] Huffman G. J., R. F. Adler, D. T. Bolvin, G. Gu, E. J. Nelkin, K. P. Bowman, Y. Hong, E. F. Stocker, and D. B. Wolff, (2007), The TRMM Multi Satellite Precipitation Analysis (TMPA): Quasiglobal, Multiyear, Combined-Sensor Precipitation Estimates at Fine Scales, *J. Hydrometeorol.*, **8**, 38-55.

